Polym. Bull. (2011) 66:363–376
DOI 10.1007/s00289-010-0336-4

ORIGINAL PAPER

Effect of compatibilizer on interfacial tension of SAN/EPDM blend as measured via relaxation spectrums calculated from Palierne and Choi–Schowalter models

M. Taheri · J. Morshedian · H. A. Khonakdar

Received: 3 May 2010 / Revised: 20 June 2010 / Accepted: 28 June 2010 /
Published online: 15 July 2010

Abstracts Morphology, interfacial tension, and stress relaxation spectra of immiscible SAN/EPDM blend and its compatibilized blend with SAN-g-EPDM (Centrex) was studied. The results showed that the morphology of the blend had a quick response to added Centrex. In the compatibilized blend with 20-wt% compatibilizer (optimized blend) having a droplet-in-matrix type of morphology, the particle sizes were reduced by a factor of 4. The power-law index of EPDM and SAN obtained 0.33 and 0.53, respectively. With increasing of compatibilizer the power-law index decreased. It meant that at the same amount of EPDM its influence in the blend was increased. Also the cross-over point of G' and G'' curves in the melt of optimized blend decreased which was attributed to increased elasticity. These observations were in good correspondence with the morphological observations. In optimized blend, the number average diameter of EPDM dispersed particles had the lowest value of about 1.8 μm. The interfacial tension of the compatibilized SAN/EPDM blend was determined from the morphological studies and the relaxation time was calculated using the Palierne and Choi-Schowalter models. The optimized blend showed the least interfacial tension about 0.306 (N/m) which was in agreement with the morphological observations.

Keywords SAN/EPDM · Compatibilizer · Relaxation time · Interfacial tension · Rheology

M. Taheri · J. Morshedian (✉) · H. A. Khonakdar
Iran Polymer and Petrochemical Institute, P.O. Box 14965/115 Tehran, Iran
e-mail: j.morshedian@ippi.ac.ir

M. Taheri
e-mail: m.taheri@ippi.ac.ir

Introduction

Many of the commodity thermoplastics lack toughness to a degree that excludes them from many applications. However, it has been found that this deficiency can be eliminated by properly blending these glassy polymers with small amount of suitable rubbery polymers. Polymeric materials made of a rubbery phase dispersed in a glassy matrix form polyblends with important applications due to their improved mechanical properties and impact strength in particular [1–4]. However, most polymers are immiscible from the thermodynamic point of view. For immiscible polymers, blending usually leads to a heterogeneous morphology [5–7]. The properties of an immiscible polymer blend are dependent on its morphology, and its morphology is strongly related to its rheological behavior. To achieve the required performance of an immiscible polymer blend, a thorough knowledge of the relationship between the morphology and the rheological behavior of the blend is essential. The morphology evolution in immiscible polymer blends affected by the rheological behavior has been a subject of intense research [8–15]. It is widely known that the presence of certain polymeric species, usually suitably chosen block or graft copolymers, can alleviate to some degree of these problems as results of their interfacial activity [16–24]. The localization of the copolymer at the interface, with the block or graft extending into their respective homopolymer phases (i.e., block A in the homopolymer A phase and vice versa) not only minimizes the contacts between the unlike segments of the copolymer and homopolymer but also displaces the two homopolymers away from the interface, thereby decreasing the enthalpy of mixing between the homopolymers [25]. The preferential localization of the copolymer at the interface has been shown by Brahimi et al. [26], Basset et al. [27], and Hosada et al. [28] for the polyethylene (PE)–polystyrene (PS) blend, polyamide (PA)–polypropylene (PP), and maleated PP–PA blends, respectively. A large number of theoretical models have been proposed to predict the rheological behavior of polymer blends. A rheological study of copolymer-modified PE–PS blend by Brahimi et al. [26] showed that the dynamic viscosity at low shear rate frequencies was very sensitive to the copolymer nature and volume fraction. The effect of copolymer modification on linear viscoelastic properties of PS–PE blend was reported by Bousmina et al. [29]. Only a few studies have investigated the rheology of SAN blends including SAN/SMA [30], compatibilized PP/SAN [23], PMMA/SAN [31], PC/SAN [32], and PA6/SAN [33] blends. Among the methods, the relaxation spectrum method and morphological properties could be used for the determination of the interfacial tension between the components of blend [34–37]. Two of the most useful models in describing linear viscoelastic behavior of polymer blends are the Palierne and Choi–Schowalter models. In our pervious study, the results showed that compatibilization of SAN/EPDM blend led to a fine morphology and improved the mechanical properties of the blend [22, 24]. In this study, objective is to determine the effect of compatibilizer on the interfacial tension between SAN and EPDM in the compatibilized SAN/EPDM blends by Palierne and Choi–Schowalter models.

Experimental

Materials and sample preparation

The polymers used in this study were obtained from commercial sources. The EPDM, Keltan 2340A, was provided by DSM Chemical Co. The SAN, APH, was provided by GhaedBasir Petrochemical Co. The graft copolymer SAN-g-EPDM, Centrex, was provided by Lanxess Co. Prior to mixing, polymeric materials were dried for at least 12 h at 80 °C in a vacuum oven. The polymers were blended in a Brabender internal mixer at 150 °C and 60 rpm. Mixing was stopped after torque stabilization. Blend of EPDM and SAN was prepared in 80/20 weight ratio to toughen SAN by EPDM. Concentrations of SAN-g-EPDM copolymer, ranging from 0 to 20 wt% with respect to the whole weight fraction of SAN/EPDM (80/20) blend were used.

Characterization

Morphological observations were taken using a scanning electron microscope (SEM Cambridge S360, England).The cryogenic specimens were dipped in liquid nitrogen for about 5 min and immediately fractured.

Mechanical properties

Both tensile and flexural tests were carried out using a universal testing machine (Instron 6025, UK), at the crosshead speeds of 50 mm/min, respectively. Impact strength was measured for notched samples, in a Zwick 5102 model instrument (Germany). At least five runs were made to report the average.

Rheological observation

The rheological behavior of EPDM, SAN, simple blend of SAN/EPDM and the ternary blend of SAN/EPDM/Centrex were studied using Rheometrics Mechanical spectrometer (RMS) parallel plate geometry, Anton Paar, MCR 300 with a gap height of 1 mm. The dynamic measurements were carried out in the linear domain for frequencies ranging from 0.1 to 600 rad/s and at three temperatures from 150 to 195 °C.

Thermal properties

TG–DSC curves of the blends were plotted by Simultaneous Thermal Analysis (STA625). All experiments were carried out in the temperature range of 25–600 °C at a heating rate of 10 °C/min.

Results and discussion

Figure 1 shows mechanical properties of the blends containing 6, 8, 10, and 20 wt% Centrex. As it is evident, there is an irregular change in stress-at-break curve from 6 to 10 wt% Centrex. This can be explained by the fact that when the amount of Centrex increases the size of dispersed phase decreases resulting in better dispersion. However, these amounts of Centrex cannot wet all the dispersed particles and thus failure occurs at interfacial places where have not been wet by Centrex. The addition of graft-copolymer as a co-agent makes an increase in the thickness of the interface to result good adhesion and efficient stress transfer [18–21, 24]. Therefore, an improved toughness–stiffness balance may be obtained in SAN/EPDM blends using 20-wt% Centrex. As it is obvious, the optimized blend shows higher stress-at-break. When the stress-at-break is low, failure could be occurred either by debonding or in an EPDM phase. In order to determine the fact, studying the results of strain-at-break can be helpful. If the strain-at-break is near the strain at break of neat EPDM, it means that failure occurs in EPDM phase. But as it can be seen in Fig. 1, the strain at break of the blend is not near to that of EPDM. Thus, the failure is because of debonding. With the addition of Centrex, the toughness of the blends increases. This clearly indicates that Centrex is able to act as a good compatibilizer to compatibilize SAN and EPDM phases.

Shear-thinning behavior of blend melt

Figure 2 shows the flow curves of pure SAN-g-EPDM and SAN/EPDM blends with different level of Centrex. It can be seen that, for all studied SAN/EPDM blends, the apparent viscosity of the melt decreases with increasing shear stress, denoting a pseudoplastic behavior. However, the pure SAN-g-EPDM shows higher pseudoplastic behavior. The power-law index of the blends determined by linear regression analysis is listed in Table 1. The power-law index of EPDM melt (0.33) is lower than that of SAN melt (0.53). When the blend melt is exposed to a shear stress, the deformation and breakup of the discrete drops give rise to a higher shear rate dependence of blend viscosity. For these blends, SAN (80 wt%) is the continuous

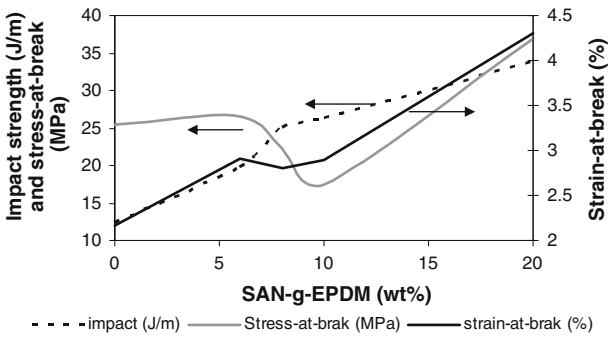

Fig. 1 Mechanical properties of the blends with different level of SAN-g-EPDM

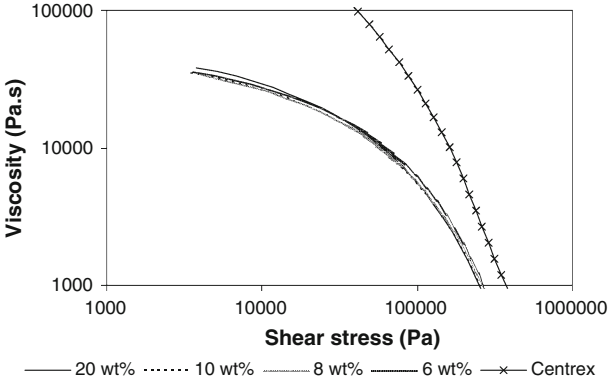

Fig. 2 Curves of melt apparent viscosity vs shear stress for SAN/EPDM blends with different level of Centrex

Table 1 Power-law index of SAN/EPDM blends for different Centrex concentration

Composition	Centrex	Compatibilized SAN/EPDM blends			
		6%	8%	10%	20%
n	0.34	0.52	0.51	0.51	0.50

phase and EPDM (20 wt%) is the dispersed phase. The results show that with increasing Centrex as compatibilizer the power-law index decreases slightly.

In Fig. 3, the rheological behavior of pure components and compatibilized blend of SAN and EPDM containing 20-wt% Centrex under the oscillating field has been depicted. As it can be seen, the viscosity of the EPDM in the melt state and its sensitivity to the changes in frequency are higher than those of the SAN. While at the low-frequency region, the elasticity of the EPDM is much higher than that of the SAN. In the case of EPDM, thanks to its rubbery nature, the entropic elasticity has a dominant role in forming its behavior. Hence by increasing the temperature, the thermal energy of the EPDM elastic chains increases. So, the movement of polymer segments and consequently interchain entanglements increases at the melt leading to a more viscous molten state. On the other hand, slippage of the rigid SAN chains over each other occurs more easily and hence viscosity and also elasticity of the SAN molten chains are lower than the EPDM. Thus, the predominant difference in the elasticity at the low frequencies is explainable. For the EPDM and the SAN, the storage modulus and loss modulus show higher values for EPDM. Also, as it is evident from the figure, the storage modulus of the neat EPDM is higher than its loss modulus which means that in the melt state its elastic behavior is more pronounced than its viscose behavior. Within the frequency range scanned, the storage and loss moduli for SAN/EPDM (80/20) blend containing 20-wt% Centrex are appeared between that of SAN and EPDM. At low frequencies, G′, G″ (Fig. 3a), and η^* (Fig. 3b) of the compatibilized blend is near to that of SAN. With increasing of frequency dynamic properties locate between SAN and EPDM. The cross-over

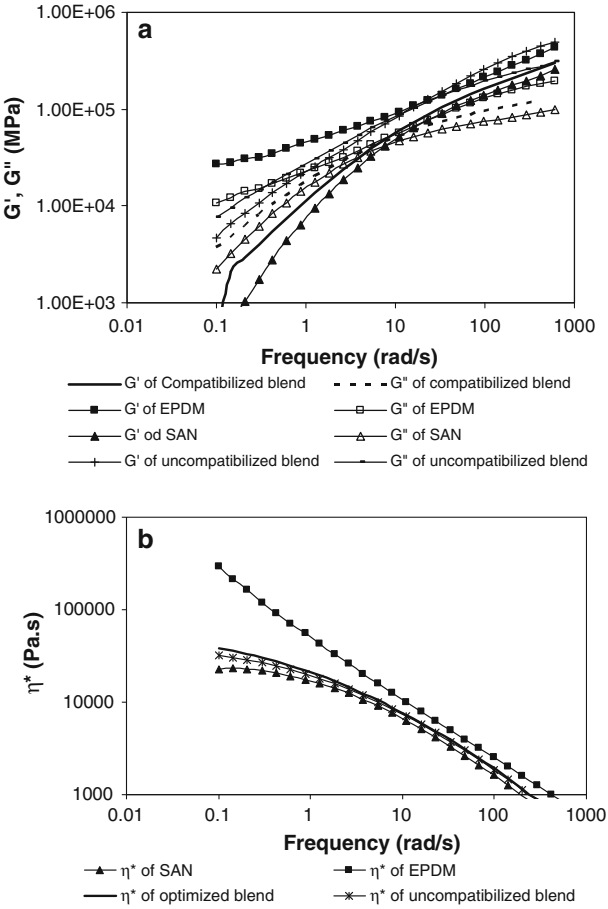

Fig. 3 Dynamic rheological behavior of EPDM, SAN uncompatibilized and optimized blend: **a** G′ and G″ and **b** η^*

point of the optimized blend (5.39 s^{-1}) is lower than uncompatibilized blend (16 s^{-1}). This can be explained by the fact that the elastic behavior of the blend is increased by adding of Centrex. As can be seen in Fig. 3b, the complex viscosity of optimized blend is higher than uncompatibilized one at low frequencies. However, the plateau region of η^* at low frequencies of optimized blend is omitted when compared to that of SAN. The optimized blend exhibits a power-law-type flow behavior with a higher viscosity and elasticity in comparison to SAN in all frequency ranges.

The morphology of the compatibilized SAN/EPDM blend with the SAN-g-EPDM (Centrex) was studied using SEM. Figure 4a–d shows micrographs of the cryogenically fractured cross-section surfaces for the compatibilized SAN/EPDM blend with the 0-, 6-, 10-, and 20-wt% Centrex, respectively. From Fig. 4, the SAN/EPDM blend shows droplet dispersion-type morphology. When the Centrex is added to the blend, the droplet size of the EPDM is decreased.

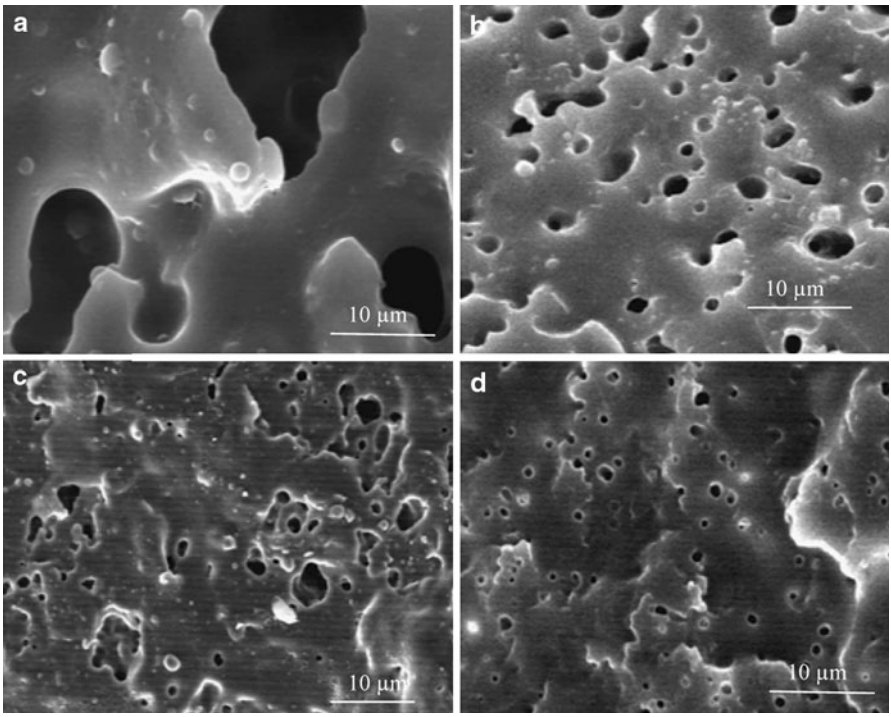

Fig. 4 SEM micrographs of the SAN/EPDM blends with Centrex, **a** uncompatibilized, **b** with 6 wt%, **c** with 10 wt%, and **d** with 20 wt%

SEM images were analyzed using Image Processing software to measure the number-average diameter (D_n), volume-average diameter (D_v), polydispersity of the particles (PD), and interparticle distance (ID) in matrix-dispersed morphologies, using Eqs. 1–4 as follows [30–32]:

$$D_n = \frac{\sum n_i \cdot D_i}{\sum n_i} \tag{1}$$

$$D_v = \frac{\sum n_i \cdot D_i^4}{\sum n_i \cdot D_i^3} \tag{2}$$

$$\mathrm{PD} = \frac{D_v}{D_n} \tag{3}$$

$$\mathrm{ID} = D_w \left[\left(\frac{\pi}{6 \cdot \phi} \right)^{1/3} \right] - 1 \tag{4}$$

where n_i is the number of particles with diameter D_i and ϕ is the volume fraction of the dispersed phase.The number-average diameter, weight-average diameter, volume-average diameter, polydispersity, and interparticle distance values for different blend compositions are shown in Table 2.

Table 2 The number-average diameter, volume-average diameter, polydispersity, and interparticle distance values for different blend compositions

Blend	D_n (μm)	D_v (μm)	PD	ID (μm)
Uncompatibilized	18	20.91	1.16	1.13
Compatibilized with 6 wt%	5.77	8.16	1.41	1.37
Compatibilized with 10 wt%	3.35	9.16	2.73	3.80
Compatibilized with 20 wt%	3.75	4.31	1.14	1.11

In Fig. 4a–d, when the Centrex is added to the SAN/EPDM blend by 6 wt%, the droplet radius of the EPDM is decreased rapidly from 9 to 2.88 μm (Table 2). When the Centrex concentration is higher than 6 wt% up to 10 wt%, it is observed that the droplet size of the EPDM is decreased slightly from 2.88 to 1.167 μm. The optimized blend when compared to the compatibilized blend with 10-wt% Centrex, the R_n increases a bit but R_v decreases. From Table 2 and Fig. 4, it is shown that the polydispersity of the dispersed particles from 6 to 20-wt% Centrex relating to the uniformity of dispersed phase distribution has the lowest value at 20-wt% Centrex (1.14). ID of the optimized blend is also minimized when compared to the other prepared blends. The efficiency of the compatibilization can be evaluated using the Favis Eq. 5, which correlates the size of the dispersed phase particles (in droplets type morphology) to the concentration of added compatibilizer [38]. It has been shown that this improvement of the morphological characteristics, from coarse to fine particles, is related to a decrease of interfacial tension between the phases [38–42]. There is an optimum concentration of compatibilizer to reduce the interfacial tension between the phases and size of dispersed phase. From Table 2, it can be seen that the average radii of the dispersed phase (both number and volume average) decrease when the compatibilizer is added to the blend. The following exponential equation (Favis equation) provides a good estimate of the dependency of the average radius on the compatibilizer concentration.

$$\frac{(R_{nc} - R_\infty)}{(R_0 - R_\infty)} = \exp(-nc) \tag{5}$$

where R_{nc} is the number average radius for a given concentration of compatibilizer, R_0 is the number average radius for a blend without compatibilizer, c is a compatibilizer concentration, and n is a constant that determines the efficiency of the compatibilizer.

Figure 5 shows the dependency of the number average radius, R_{nc}, on the compatibilizer concentration for both experimental and analytical data (by exponential regression). The dotted line is plotted based on experimental data given in Table 2. This line cannot be compared with Favis equation. This equation has an exponential form thus to determine the optimum compatibilizer concentration, the black line is plotted via exponential regression from data shown in Table 2. Now the exponential equation based on experimental data (the black line) can be compared to Favis exponential equation.

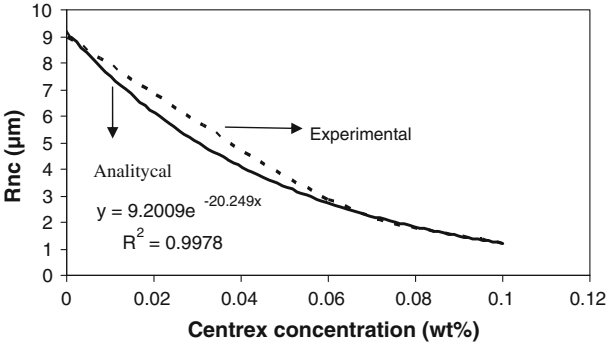

Fig. 5 Dependency of the number average radius to the compatibilizer concentration

By comparing the slope of analytical exponential curve with that of Favis equation, the quantity of $(R_0–R_\infty)$ is obtained to be 9.2 µm. As mentioned above, R_0 was about 9 µm. It means that the constant value for this blend (R_∞) can be calculated to be −0.2. Jerome and co-workers [43] showed that effective toughening occured at an optimum particle size of 0.1–1 µm for EPDM droplets in SAN. If we enter 9 and −0.2 for the values of R_0 and R_∞, and both 0.1 and 1 for the values of c in the Favis Eq. 5 the optimum compatibilizer concentration in this blend ranges from 10 to 17 wt% which is in close agreement with our chosen concentrations, i.e., 10 and 20 wt%.

Figure 6 shows the weighted relaxation spectrum ($\tau\ H(\tau)$) versus the relaxation time (τ) for the EPDM and SAN. The weighted relaxation spectrum was obtained from the storage modulus data in Fig. 3a. The relaxation spectrum, $H(\tau)$, can be determined using the Tschoegle approximation [44] as shown in Eq. 6:

$$H(\tau) = G'\Big[\mathrm{d}\log G'/\mathrm{d}\log\omega - 1/2(\mathrm{d}\log G'/\mathrm{d}\log\omega)^2 - (1/4.606)\mathrm{d}^2\log G'\Big/\mathrm{d}(\log\omega)^2\Big]_{1/\omega=\pi/\sqrt{2}} \quad (6)$$

where ω is the frequency and τ is the relaxation time. It is important to know the relaxation time of the components to investigate the compatibilization effect on the blends. From Fig. 6, it is observed that the relaxation time of EPDM is 0.567 s and two relaxation times at 0.282 and 1.14 s are resulted for SAN.

Figure 7 shows the weighted relaxation spectrum of the SAN/EPDM uncompatibilized blend and compatibilized with 6, 8, 10, and 20 wt% of SAN-g-EPDM (Centrex). The relaxation times deduced from this figure are summarized in Table 3. For the uncompatibilized blend, three relaxation peaks are observed at about 0.55, 1.91, and 3.23 s. The first peak (0.55 s) and the second peak (1.91 s) are related to the phases of the components. The new peak at 3.23 s is associated with the contribution of the relaxation time of the interface of the EPDN and SAN blend [45, 46]. As shown in Fig. 7, when Centrex is added to the blend up to 8 wt%, the new peak is omitted and the second relaxation time is decreased from 1.91 to 0.955 s (Table 3). For the blend with 10- and 20-wt% Centrex, the second relaxation time is increased. It can be concluded that Centrex (SAN-g-EPDM) is

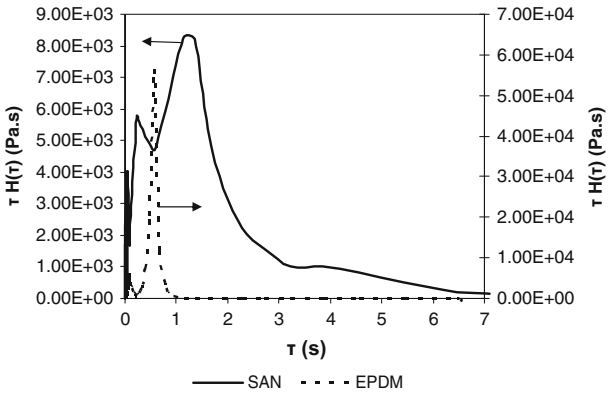

Fig. 6 Weighted relaxation spectrum of the EPDM and SAN

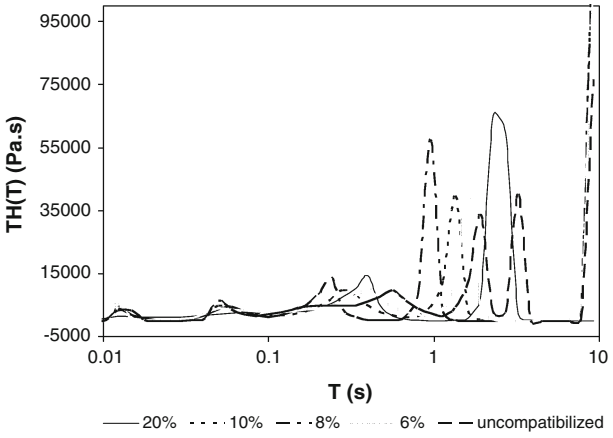

Fig. 7 Weighted relaxation spectrum of SAN/EPDM (80/20) blend with different level of compatibilizer

Table 3 Relaxation times (τ) for the compatibilized blends with different Centrex content

Centrex (wt%)	0	6	8	10	20
τ_1	0.55	0.4	0.237	0.280	0.4
τ_2	1.91	1.61	0.955	1.35	2.28
τ_3	3.23	–	–	–	–

segregated as the third phase. Similar results were observed by Macaubas and Demarquette [46] for the PP–PS–SBS blend.

Interfacial properties of immiscible polymer blends rely on a key principle that such materials are emulsions in the molten state. The process during which a deformed particle is regaining its spherical form is called the form relaxation process. This process has a characteristic relaxation time. To get the interfacial

tension, Taylor extended Einstein's analysis to include the case of emulsions composed of spherical particles of a Newtonian liquid in another immiscible Newtonian liquid and proposed an equation. Choi and Schowalter [47] extended Taylor's theory and introduced the deformability of the dispersing particles. Palierne [36] proposed an emulsion model that took into account the particle size distribution and the interface properties. Palierne emulsion model has been widely used to quantitatively describe the linear viscoelastic properties of polymer blends and to derive the interfacial tension between their phases [37]. To get the interfacial tension in the SAN/EPDM blend, we used Palierne emulsion model shown in Eq. 7. The interfacial relaxation time is expressed in Eq. 7 as:

$$\tau = \left(\frac{R_v \eta_m}{4\alpha}\right) \frac{(19K+16)(2K+3-2\phi(K-1))}{10(K+1)-2\phi(5K+2)} \tag{7}$$

where η_m is the viscosity of the matrix, α is the interfacial tension of the blend, ϕ is the volume fraction and is the volume-average radius of the dispersed phase, and $K = \eta_d/\eta_m$ is the zero shear viscosity ratio of the droplet and matrix. Interfacial tension was also obtained from Choi–Schowalter model shown in Eq. 8. The form relaxation time (τ_2) (Table 3) and the interfacial tension (α) are related as follows: Applying Eqs. 7 and 8 to the SAN/EPDM blend, the interfacial tension can be obtained for each model.

$$\tau = \left(\frac{R_v \eta_m}{\alpha}\right) \frac{(19K+16)(2K+3)}{40(K+1)} \times \left[1 + \phi \frac{5(19K+16)}{4(K+1)(2K+3)}\right] \tag{8}$$

Table 4 shows the interfacial tension of the compatibilized SAN/EPDM blends calculated from the Palierne and the Choi–Schowalter models. η_m and K were obtained from Fig. 3b. R_v and τ were obtained from SEM images, Tables 2 and 3, respectively. From the Palierne model, the interfacial tension of the blends shows minimum value (0.31 N/m) in the 20-wt% Centrex content, which suggests that compatibility, is increased with the copolymer content. For the Choi and Schowalter model, the interfacial tension shows also a minimum value (0.36 N/m) at 20-wt% Centrex, which represents similar trend with the result obtained by Palierne model. The results of the interfacial tension (α) and form relaxation time (τ), Table 3, are consistent with the results obtained from the morphological studies of the SAN/EPDM blends (Fig. 4). As mentioned before the blend containing 20-wt% Centrex shows better distribution and uniform dispersion due to the compatibilization effect of Centrex.

Another approach to investigate the miscibility and the morphology of the blend via rheological data is making use of the Cole–Cole diagram depicted in Fig. 8. In

Table 4 Interfacial tension of the blends calculated from the Palierne and the Choi–Schowalter models

Centrex (wt%)	R_v	α_p (N/m)	α_{Ch-S} (N/m)
0	10.45	1.05	1.24
6	4.08	0.82	0.97
10	4.58	1.10	1.31
20	2.15	0.31	0.36

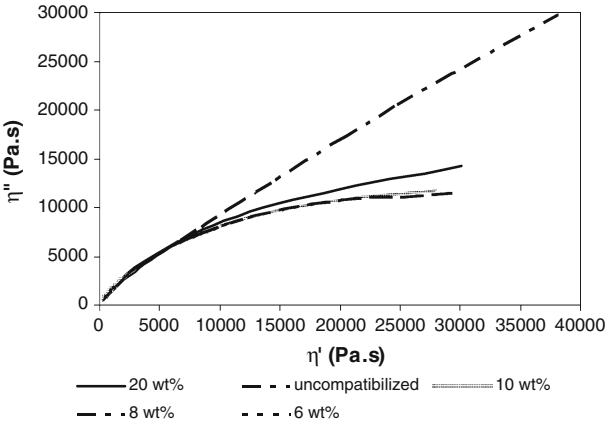

Fig. 8 Cole–Cole plot of compatibilized SAN/EPDM blends at different level of Centrex

this diagram, n'' is plotted versus η'. As can be seen the blends with compatibilizer show semi circle shapes. In optimized blend, the diagram has a close form to a semi circle, but has a little deviation. This is an indication for the immiscibility besides owning a good compatibility. These results agree with the previous rheological and morphological observations.

Conclusion

In this study, the relationship between morphological observations, rheological, and mechanical properties of compatibilized SAN/EPDM blends with Centrex compatibilizer were studied. Uncompatibilized and compatibilized blends showed a dispersion of droplets of minor phase in a matrix type of morphology. Addition of Centrex to the dispersed phase of the blend was found to reduce the size of the dispersed phase particles. At 20-wt% Centrex content, the droplet size of the EPDM showed the least value (1.87 μm) in the SAN/EPDM (80/20) blend. The power-law indices of the blends determined by linear regression analysis showed that with increasing Centrex decreased slightly. The rheological measurements of the neat EPDM showed non-Newtonian behavior, while those of the neat SAN indicated a Newtonian behavior in low frequencies. The values of G′, G″, and η^* of the optimized blend were read between those of SAN and EPDM and at low frequencies were closer to SAN. The G′–G″ cross-over point for this blend was lower than that of uncompatibilized blend. This explained that the elastic behavior of the blend is increased. This result is consistent with the result obtained from power-law index to confirm more elasticity. Favis equation was used to determine the optimum compatibilizer concentration. It predicted that at 0.17 wt% of Centrex, the size of dispersed phase would be minimum. This concentration was near to maximum chosen concentration (20 wt%) in this study. The weighted relaxation spectra of the blends were also studied. They were found to be a combination of the weighted relaxation spectra of the pure phases of the blend and an additional relaxation time

associated with the interface. From the weighted relaxation spectrum of the SAN/EPDM blend with Centrex, the interfacial tension of the blends was determined. It was also calculated using the Palierne and the Choi–Schowalter models which showed minimum value at 20-wt% Centrex. The results of interfacial tens ion were consistent with the results obtained from the rheological and morphological studies of the blends suggesting increased compatibility at 20-wt% Centrex. Moreover for this blend the mechanical properties, including the tensile and impact strength gained the highest values.

References

1. Utracki LA (2003) Polymer blends handbook. Kluwer Academic, Dordrecht
2. Dekkers MEJ (1994) Artificial polymer lattices in core-shell form and method of preparation. US Patent 5356955
3. Maciel A, Salas V, Manero O (2005) PP/EVA blends: mechanical properties and morphology. Effect of compatibilizers on the impact behavior. Adv Polym Technol 24:241–252
4. Teh JW, Rudin A, Keung JC (1994) A review of polyethylene-polypropylene blends and their compatibilization. Adv Polym Technol 13:1–23
5. Kroeze E, Brinke G, Hadziioannou G (1997) Compatibilization of low-density polyethylene/polystyrene blends by segmented EB(PS-block-EB) n block copolymers. Polym Bull 38:203–210
6. Mıh M, Aras L, Alkan C (2003) Compatibilization of poly(2, 6-dimethyl-l, 4-phenylene oxide) and Poly(2, 6-dichloro-l, 4-phenylene oxide) with sulfonated polystyrene and its Na and Zn-neutralized ionomers. Polym Bull 50:123–212
7. Ao Y, Tang K, Xu N, Yang H, Zhang H (2007) Compatibilization of PP/SEBS-MAH blends by grafting glycidyl methacrylate onto polypropylene. Polym Bull 59:161–298
8. Özen l, lu M (2009) Morphology of poly(ethylene terephthalate) blends: an analysis under real processing conditions by rheology and microscopy. Adv Polym Technol 28:173–184
9. Chandramouli K, Jabarin SA (1995) Morphology and property relationships in ternary blends of polyethylene/polyamide-6/compatibilizing agents. Adv Polym Technol 14:35–46
10. Varanasi PP, Ryan ME, Stroeve P (1994) Experimental study on the breakup model of viscoelastic drops in uniform shear flow. [J]. Ind Eng Chem Res 33:1858–1866
11. Huneault MA, Shi H, Utracki LA (1995) Development of polymer blend morphology during compounding in a twin-screw extruder. Part IV: a new computational model with coalescence. J Polym Eng Sci 35:115–127
12. Gonzalez-nunez R, Kee DD, Favis BD (1996) The influence of coalescence on the morphology of the minor phase in melt-drawn polyamide-6/HDPE blends. J Polym 37:4689–4693
13. Bourry D, Favis BD (1998) Morphology development in a polyethylene/polystyrene binary blend during twin-screw extrusion. J Polym 39:1851–1856
14. Testa C, Sigillo I (2001) Morphology evolution of immiscible polymer blends in complex flow fields. J Polym 42:5651–5659
15. Gonzalez-nunez R, Arellano M, Moscoso FJ, Favis BD (2001) Determination of a limiting dispersed phase concentration for coalescence in PA-6/HDPE blends under extensional flow. J Polym 42:5485–5489
16. Chaintore O, Trossarelli L, Lazzari M (1998) Compatibilization effects in the thermal degradation of blends containing SAN and EPDM polymers. Polymer 39(13):2777–2781
17. Hoang T, Trung T, Yoo G, Ahn JH, Zin W (2001) Compatibilization of SAN/EPDM blends by grafting EPDM with methyl methacryl. Bull Korean Chem Soc 22:1037–1040
18. Hrnjak Z, Jelcic Z, Kovacevic V (2002) Molecular and morphological characterization of immiscible SAN/EPDM blends field by Nano filler. Macromol Mater Eng 287:684–692
19. Qu X, Sh Shang, Liu G (2004) Effect of the addition of acrylonitrile/EPDM/Styrene graft copolymer on the morphology-properties relationships in SAN/EPDM blends. J Appl Polym Sci 91:1685–1697
20. Zeng Z, Wang L, Cai T (2004) Synthesis of high rubber styrene-EPDM-acrylonitrile graft copolymer and its toughening effect on SAN. J Appl Polym Sci 94:416–423

21. Kratofil LJ, Pticek A, Hrnjak-Murgic Z (2007) Compatibilization effects in SAN/EPDM blends prepared by reactive extrusion. J Elastomeric Plastics 39:371–382
22. Taheri M, Morshedian J, Esfandeh M (2006) Reactive compatibilization of SAN/EPDM blend and study of the parameters affecting its properties. Iran Polym J 15:955–965
23. Sung YT, Han MS, Hyun JC (2003) Rheological properties and interfacial tension of PP/SAN blend containing compatibilizer. Polymer 44:1681–1687
24. Taheri M, Morshedian J, Esfandeh M (2008) Compatibilization and properties of SAN/EPDM blends with the addition of coagents. J Appl Polym Sci 110:753–760
25. Wenchun H, Koberstein JT, Lingelser JP, Gallot Y (1995) Interfacial tension reduction in polystyrene/poly(dimethylsiloxane) blends by the addition of poly(styrene-b-dimethylsiloxane. Macromolecules 28:5209
26. Brahimi B, Ait-Kadi A, Ajji A, Jerome R, Fayt R (1991) Effect of diblock copolymers on dynamic mechanical properties of polyethylene/polystyrene blends. J Rheol 35:1069
27. Basset D, Lecerf F, Martin J.M (1991) In Française de Chimie Société: Colloque Francais-Iberique de Microsopie Electonique, 2–5 July
28. Hosada S, Kojima K, Kanda Y, Aoyagi M (1991) Polym Netw Blends 1:51
29. Bousmina M, Bataille P, Sapieha S, Schreiber HP (1995) Comparing the effect of corona treatment and block copolymer addition on rheological properties of polystyrene/polyethylene blends. J Rheol 39:499
30. Pathak J, Gurp MV (2000) Rheology of a miscible blend of SAN and SMA. J Appl Polym Sci 78:1245–1249
31. Zuo M, Zheng Q (2006) Phase morphologies and viscoelastic relaxation behaviors for an LCST-type polymer blend composed of poly(methyl methacrylate) and poly[(a-methyl styrene)-co-arylonitrile]. Macromol Chem Phys 207:1927–1937
32. Kang EA, Kim JH, Kim CK, Rhece HW (2000) The effects of PC-PMMA block copolymer on the compatibility and interfacial properties of PC/SAN blends. Polym Eng Sci 40:11
33. Sailer Ch, Handge UA (2007) Influence of reactive compatibilization on the melt flow properties and morphology of polyamide 6/styrene-acrylonitrile blends. Macromol Symp 254:217–225
34. Khonakdar HA, Jafari SH, Yavari A, Asadinezhad A, Wagenknecht (2005) Rheology morphology and estimation of interfacial tension of LDPE/EVA and HDPE/EVA blends. Polym Bull 54(1–2): 75–84
35. Gleinser W, Braun H, Friedrich Chr, Cantow HJ (1994) Correlation between rheology and morphology of compatibilized immiscible blends. Polymer 35:128–135
36. Palierne JE (1990) Linear rheology of viscoelastic emulsions with interfacial tension. Rheol Acta 29:204–214
37. Shi D, Hu GH, Ke Z, Li RKY (2006) Relaxation behavior of polymer blends with complex morphologies: Palierne emulsion model for uncompatibilized and compatibilized PP/PA6 blends. Polymer 47:4659–4666
38. Favis BD (1994) Phase size/interface relationships in polymer blends: the emulsification curve. Polymer 35:1552–1555
39. Chapleau N, Favis BD, Carreau PJ (1998) Measuring the interfacial tension of polymers in the presence of an interfacial modifier: migrating the modifier to the interface. J Polym Eng Sci B 36:1947–1957
40. Lepers JC, Favis BD (1999) Interfacial tension reduction and coalescence suppression in compatibilized polymer blends. AIChE J 45:887–895
41. Demarquette NR, Kamal MR (1998) Influence of maleation of polypropylene on the interfacial properties between polypropylene and ethylene-vinyl alcohol copolymer. J Appl Polym Sci 70:75–87
42. Garmabi H, Demarquette NR, Kamal MR (1998) Effect of temperature and compatibilizer on interfacial tension of PE/PA-6 and PP/EVOH. Int Polym Process XIII(2):183–191
43. Albert B, Jerome R, Teyssie Ph (1986) Investigation of miscibility by spectroscopic methods IV. How far is poly(vinyl chloride) miscible with s-poly(methyl methacrylate) and poly(styrene-co-acrylonitrile)? An answer from nonradiative energy transfer. J Polym Sci A 24:551–558
44. Tschoegl NW (1989) The phenomenological theory of linear viscoelastic behavior. Springer, Berlin
45. Moan M, Huitric J, Mederic P, Jarrin J (2000) Rheological properties and reactive compatibilization of immiscible polymer blends. J Rheol 44:1227
46. Macaubas PHP, Demarquette NR (2001) Morphologies and interfacial tensions of immiscible polypropylene/polystyrene blends modified with triblock copolymers. Polymer 42:2543
47. Choi SJ, Schowalter WR (1975) Rheological properties of nondilute suspensions of deformable particles. Phys Fluids 18:420